

A study on the topographical and geotechnical effects in 2-D soil-structure interaction analysis under ground motion

Oğuz Akın Düzgün* and Ahmet Budak

Department of Civil Engineering, Engineering Faculty, Ataturk University, 25240 Erzurum, Turkey

(Received January 5, 2010, Revised May 5, 2011, Accepted November 7, 2011)

Abstract. This paper evaluates the effects of topographical and geotechnical irregularities on the dynamic response of the 2-D soil-structure systems under ground motion by coupling finite and infinite elements. A numerical procedure is employed, and a parametric study is carried out for single-faced slope topographies. It is concluded that topographic conditions may have important effects on the ground motion along the slope. The geotechnical properties of the soil will also have significantly amplified effects on the whole system motion, which cannot be neglected for design purposes. So, dynamic response of a soil-structure systems are primarily affected by surface shapes and geotechnical properties of the soil. Location of the structure is another parameter affecting the whole system response.

Keywords: soil-structure interaction; finite elements; infinite elements; elastodynamics; topography; site effects; ground motion

1. Introduction

It has been well understood that the geotechnical and topographical features have a significant influence on strong ground motion. This fact has an important effect on the dynamic response of the structures such especially as bridges and dams during strong seismic events. The seismic effects of topographic irregularities have been repeatedly shown to be detrimental to structures. In the event of a strong earthquake, structures located at the top of hills, ridges or canyons, suffer more considerable damage than those located at the base. Besides, structures standing near the edge of irregular topographies, such as cliffs, are affected significantly more than those at some distance from the edge. Severe structural damage due to topographic features has been observed in numerous earthquakes: in Tokachi-oki (Japan) 1968, San Fernando (USA) 1971, Friuli (Italy) 1976, Miyagiken-oki (Japan) 1978, Irpinia (Italy) 1980, Chile 1985, Eje-Cafetero (Colombia) 1998, Athens (Greece) 1999, and Bingöl (Turkey) 2003. (See details in Ohtsuki and Harumi 1983, Ohtsuki *et al.* 1984, Celebi 1987, Kawase and Aki 1990, Gazetas *et al.* 2002, Assimaki *et al.* 2005). It has been considered that such severe structural damage is due to the large amplification of seismic waves associated with local topography and surface soil properties (Ohtsuki and Harumi 1983, Ohtsuki *et al.* 1984).

*Corresponding author, Ph.D. Student, E-mail: aduzgun@atauni.edu.tr

There are a large number of analytical and numerical studies which have provided supporting evidence of the significance of topographical effects. The finite difference method is used by Boore (1972) to model site effects for P-SV waves propagation in arbitrary topographical features. Analytical solutions are obtained for SH wave scattering for semi-cylindrical canyons by Trifunac (1973) and for semi-elliptical canyons by Wong and Trifunac (1974). The scattering and diffracting SH wave problems are extended by Wong and Jennings (1975) to arbitrarily-shaped canyons under ground motion by using boundary integral techniques and Fourier transforms. The diffraction of P, SV and Rayleigh waves by a circular canyon and an elliptical canyon is studied in Wong (1979). Effects of topographical and subsurface inhomogeneities are examined by Ohtsuki and Harumi (1983) on seismic SV waves and by Ohtsuki *et al.* (1984) on seismic Rayleigh waves by using the hybrid method combining a particle model with finite elements. Effects of canyon topographies and geological conditions on strong ground motion are studied in Zhang and Zhao (1988) by using coupling finite and infinite elements. A procedure is presented by Avilés and Pérez-Rocha (1998) for representing the site effects and soil-structure interaction in alluvial valleys by using the one-dimensional (1-D) theory of shear wave propagation. An experimental study carried out in 1993 near Corinth in Greece is presented in LeBrun *et al.* (1999) to investigate a scale effect of the dimensions of the hill, by comparing the results of an experiment carried out in 1992 around Sourpi and to compare the observed amplification level with those already reported in the literature. Complex site effects are studied by Chávez-García and Faccioli (2000) to explore how to modify seismic spectra in order to take into account site effects of a two-dimensional (2-D) nature on sine-shaped sedimentary valleys. They concentrated on evaluating the additional amplification that 2-D site effects produced on ground motion. Gazetas *et al.* (2002) carried out a case study to determine topography and soil effects in Adámes region during 1999 Parnitha (Athens) Earthquake. Havenith *et al.* (2003) examined the effects of various geological factors on the seismic ground motion, such as the presence of surface layers, 2-D and 3-D topography and of a fault zone located at the bottom of the hill. A case-study is carried out by Assimaki *et al.* (2005) to illustrate the role of material inhomogeneity, soil-structure interaction and local stratigraphy in altering the energy mechanism at the different topographies. Another case-study is carried out by Stewart and Sholtis (2005) to determine the effects of topography and geological amplification on single-faced slopes. Gatmiri and Arson (2008) carried out a parametric study to quantify the site effects in 2-D sedimentary valleys by using an optimized 2-D boundary and finite element method. Zulkifli and Ruge (2009) introduced a matrix-valued algebraic formulation in the frequency domain and a corresponding equation in the time domain for soil-structure interaction problem with a layered soil excited in transient loading to evaluate the radiation damping. Chore *et al.* (2010) carried out a parametric study to determine the effect of soil structure interaction on a single-storey, two-bay space frame resting on a pile group embedded in the cohesive soil with flexible cap by using 3-D finite element analysis. There is, however, a need of a better understanding of influence of soil-structure interaction associated with local topographic irregularities on both strong ground motion and dynamic response of structures.

In this paper, effects of topography and soil properties on the dynamic response of 2-D soil-structure systems under ground motion are investigated. The systems consist of a structure and a soil layer which include only one slope. A numerical procedure is employed to evaluate the whole system response. In the numerical treatment, finite and infinite elements with three wave types (Yerli *et al.* 1998) are used. This infinite elements type represents the characteristics of pressure (P), shear (S) and Rayleigh waves at the same time. In the modeling of the structure and near soil

region, finite elements are used, while far soil region is modeled by infinite elements. The soil region is assumed to be homogeneous, isotropic and viscoelastic layer. For the ground motion data acting horizontally on the soil-rigid base interface, Ricker-Wavelet is chosen. A parametric study is carried out to determine the effects of topography and soil properties, on the response of soil and the structure. Special attention is paid to evaluate the dynamic response of the structure due to the amplification of waves by the local soil properties and the amplification due to the topographical irregularities. The formulation is performed in the Laplace transform domain. Solution in the time domain is obtained by using Durbin's numerical inverse Laplace transform technique (Durbin 1974).

2. Equation of motion in Laplace transform domain

In the 2-D soil-structure interaction analysis under ground motion, formulations are made depending on relative displacements. Equilibrium equations for 2-D problems under ground motion are given by

$$\begin{aligned}\frac{\partial \sigma_x}{\partial x} + \frac{\partial \tau_{xy}}{\partial y} + f_x - \rho \frac{\partial^2 u}{\partial t^2} &= 0 \\ \frac{\partial \tau_{xy}}{\partial x} + \frac{\partial \sigma_y}{\partial y} + f_y - \rho \frac{\partial^2 v}{\partial t^2} &= 0\end{aligned}\quad (1)$$

where u and v are total displacement components and defined as

$$\begin{aligned}u &= u_r + u_g \\ v &= v_r + v_g\end{aligned}\quad (2)$$

In Eq. (2), u_g and v_g are displacements due to ground motion, undisturbed by soil-structure interaction; u_r and v_r are relative displacements of any point in the soil-structure system with respect to that of the ground surface. When Eq. (2) is substituted in Eq. (1), equilibrium equations are obtained as follows

$$\begin{aligned}\frac{\partial \sigma_x}{\partial x} + \frac{\partial \tau_{xy}}{\partial y} + f_x - \rho \frac{\partial^2 u_r}{\partial t^2} - \rho a_{gx} &= 0 \quad \left(a_{gx} = \frac{\partial^2 u_g}{\partial t^2} \right) \\ \frac{\partial \tau_{xy}}{\partial x} + \frac{\partial \sigma_y}{\partial y} + f_y - \rho \frac{\partial^2 v_r}{\partial t^2} - \rho a_{gy} &= 0 \quad \left(a_{gy} = \frac{\partial^2 v_g}{\partial t^2} \right)\end{aligned}\quad (3)$$

where a_{gx} and a_{gy} are horizontal and vertical ground accelerations, respectively. Now, Applying Laplace transformation (Yerli *et al.* 1998) to Eq. (3) and integrating over an element multiplying by weighting factors, afterwards Galerkin's approach is employed, the governing differential equations are expressed in integral form as

$$h_e \int_{A_e} \{ \delta \bar{\epsilon} \}^T \{ \bar{\sigma} \} dA_e + s^2 h_e \int_{A_e} \rho \left\{ \frac{\delta \bar{u}_r}{\delta \bar{v}_r} \right\}^T \left\{ \bar{u}_r \right\} dA_e =$$

$$h_e \int_{A_e} \left\{ \frac{\delta \bar{u}_r}{\delta \bar{v}_r} \right\}^T \left\{ \bar{f}_x \right\} dA_e + h_e \int_S \left\{ \frac{\delta \bar{u}_r}{\delta \bar{v}_r} \right\}^T \left\{ \bar{t}_x \right\} dS - h_e \int_{A_e} \rho \left\{ \frac{\delta \bar{u}_r}{\delta \bar{v}_r} \right\}^T \left\{ \bar{a}_{gx} \right\} dA_e \quad (4)$$

where h_e is element thickness, ρ is mass density and s is Laplace transform parameter. Overbar represents the Laplace transform of related quantity. Eq. (4) is the usual virtual work principle in the Laplace transform domain. In the numerical treatment, by using finite element approximation, the system equations of motion in the Laplace transform domain are obtained as

$$([\bar{K}] + s^2[\bar{M}])\{\bar{U}\} = \{\bar{P}\} \quad (5)$$

in which $[\bar{K}]$ and $[\bar{M}]$ are system stiffness and mass matrices, $\{\bar{P}\}$ is system load vector and $\{\bar{U}\}$ is system displacement vector that contains all of the nodal displacements. In the presence of viscous damping in the material, the material constants in the material matrix are to be multiplied by $(1 + \zeta s)$. Here, ζ is damping coefficient.

3. Formulations of finite and infinite elements

In dealing with the interaction problems with geometrical irregularities and different geological properties, a coupling system of finite and infinite elements has proved to be an effective procedure (Zhang and Zhao 1987, 1988). In this study, a standard eight-node isoparametric, quadratic plane element is used as the finite element. Fig. 1 shows the eight-node isoparametric, quadratic finite element. The chosen finite element's formulations are well-known. For this reason, the formulations need not be discussed in detail, only interpolation functions are given as (Reddy 1993)

$$\begin{aligned} N_i &= \frac{1}{4}(1 + \xi\xi_i)(1 + \eta\eta_i)(\xi\xi_i + \eta\eta_i - 1) \quad (\text{corner nodes}) \\ N_i &= \frac{1}{2}(1 - \xi^2)(1 + \eta\eta_i) \quad (\text{side nodes, } \xi_i = 0) \\ N_i &= \frac{1}{2}(1 + \xi\xi_i)(1 - \eta^2) \quad (\text{side nodes, } \eta_i = 0) \end{aligned} \quad (6)$$

For the discretization of the far soil region, infinite elements that include three different wave types (P , S and Rayleigh waves) have been used. Fig. 2 shows the infinite elements adequate to represent the propagation of three wave types. The shape functions of dynamic infinite elements are constructed by using a wave-propagation function that represents the amplitude attenuation and phase delay in the direction extending to infinity. The mapping functions of the infinite elements are given as (Zhang and Zhao 1987)

$$\begin{aligned} M_1 &= \frac{1}{2}(\xi - 1)(\eta - 1) \\ M_2 &= 0 \\ M_3 &= \frac{1}{2}(1 - \xi)(\eta + 1) \end{aligned}$$

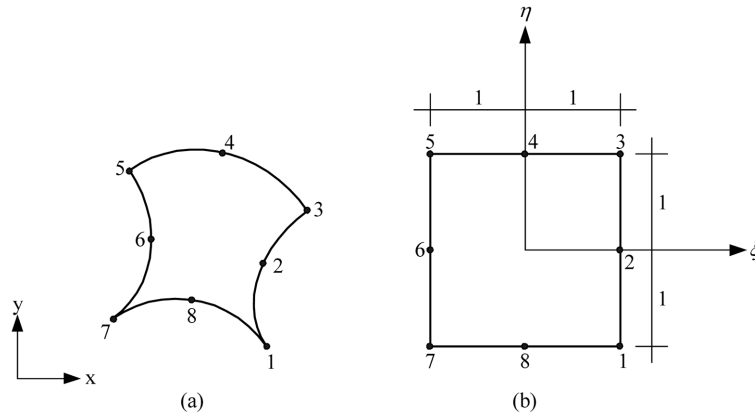


Fig. 1 Eight-node isoparametric finite element

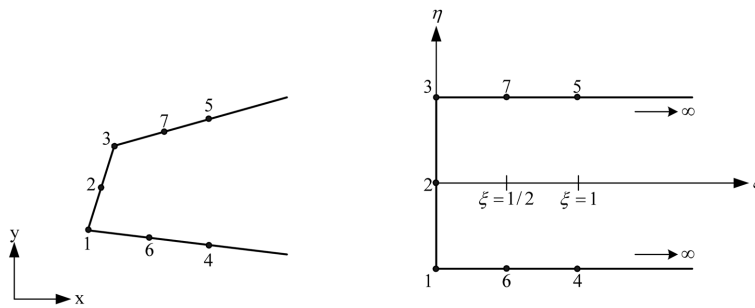


Fig. 2 Infinite element with three wave types

$$M_4 = \frac{1}{2} \xi(1-\eta)$$

$$M_5 = \frac{1}{2} \xi(1+\eta) \quad (7)$$

In the Laplace transform domain, the horizontal (\bar{u}) and vertical (\bar{v}) displacement fields of the infinite element can be written as

$$\bar{u} = \sum_{i=1}^7 \bar{N}_i \bar{u}_i \quad \bar{v} = \sum_{i=1}^7 \bar{N}_i \bar{v}_i \quad (8)$$

where N_i : displacement shape functions of the infinite element, and they can be expressed as

$$\bar{N}_1(\xi, \eta, s) = \bar{P}_1(\xi, s) \left[\frac{1}{2} \eta(\eta-1) \right]$$

$$\bar{N}_2(\xi, \eta, s) = \bar{P}_2(\xi, s)(1-\eta^2)$$

$$\begin{aligned}
\bar{N}_3(\xi, \eta, s) &= \bar{P}_3(\xi, s) \left[\frac{1}{2} \eta (\eta + 1) \right] \\
\bar{N}_k(\xi, \eta, s) &= \bar{P}_k(\xi, s) \left[\frac{1}{2} (1 - \eta) \right] \quad k = 4, 6 \\
\bar{N}_k(\xi, \eta, s) &= \bar{P}_k(\xi, s) \left[\frac{1}{2} (1 + \eta) \right] \quad k = 5, 7
\end{aligned} \tag{9}$$

where $P_k(\xi, s)$ is the wave-propagation function. Based on the derivation for the harmonic infinite elements given by Zhang and Zhao (1987), the wave-propagation functions can be approximately represented by the superposition of plane waves. Thus, their general form in the Laplace transform domain is expressed by Yerli *et al.* (1998) as

$$P_k(\xi, s) = ae^{-(\alpha + \beta_1)\xi} + be^{-(\alpha + \beta_2)\xi} + ce^{-(\alpha + \beta_3)\xi} \quad \beta_k = \frac{s}{c_k} L \tag{10}$$

where α : decay parameter; c_k : wave velocities and a, b, c are undetermined constants. To determine the constants a, b and c , detailed formulations are given in Yerli *et al.* (1998) by using Eq. (8).

Calculation of the infinite element stiffness and mass matrices is performed numerically. For the finite direction, the usual Gauss-Legendre integration technique is used. But infinite integrals are evaluated by using Newton-Cotes numerical integration scheme (Bettess and Zienkiewicz 1977).

4. Parametric studies

Effects of topographic irregularities and soil properties on the dynamic response of the 2-D soil-structure systems which include only one slope are evaluated under ground motion. Diverse shapes of soil-structure systems are studied. A schematic representation of the numerical models is shown in Fig. 3. Here, T0 is the reference soil-structure system which has a regular surface shape. Other topographic shapes are considered as $\alpha = 90^\circ$ (T1); $\alpha = 75^\circ$ (T2); $\alpha = 60^\circ$ (T3); $\alpha = 45^\circ$ (T4) and $\alpha = 30^\circ$ (T5), where α is slope angle. In the soil-structure systems, the structure is modeled as a solid block to determine the global dynamic response of the structure with mass density $\rho_{str} = 2.4 \text{ t/m}^3$, accounting for the macroscopic properties of the structural system, and Poisson's ratio $\nu = 0.20$ and modulus of elasticity $E_{str} = 30000 \text{ MPa}$; its height is 12 m. for all simulations, corresponding to a 4-story building with 3 m. mean story-to-story spacing and its width is considered as 5 m. The soil region is assumed as homogeneous, isotropic and viscoelastic layer. The height of soil layer is assumed constant in all simulations. Underlying rock is considered as rigid base. It is noted that in all simulations, no relative displacement is allowed at the soil-structure and soil-rock interface. Reference soil properties are considered as mass density $\rho_s = 2.0 \text{ t/m}^3$, Poisson's ratio $\nu = 0.35$ and modulus of elasticity $E_s = 200 \text{ MPa}$. Three different soil types are taken into account, i.e., Soil Type I ($G1 / G = 1$), Soil Type II ($G2 / G = 0.75$) and Soil Type III ($G3 / G = 0.5$), where G and $G\#$ represent shear modulus of reference soil and of other soil types, respectively. Because of the viscous damping effect is not under particular interest, it is assumed that all soil types have 5% constant viscous damping ratio. On the other hand, the material properties are not crucial because

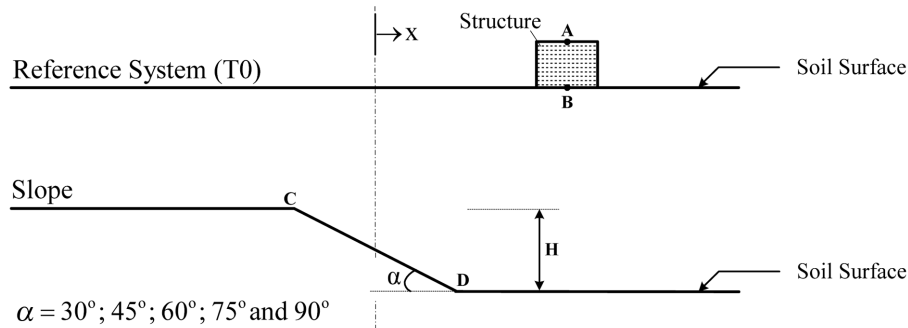


Fig. 3 Configurations of the soil-structure systems

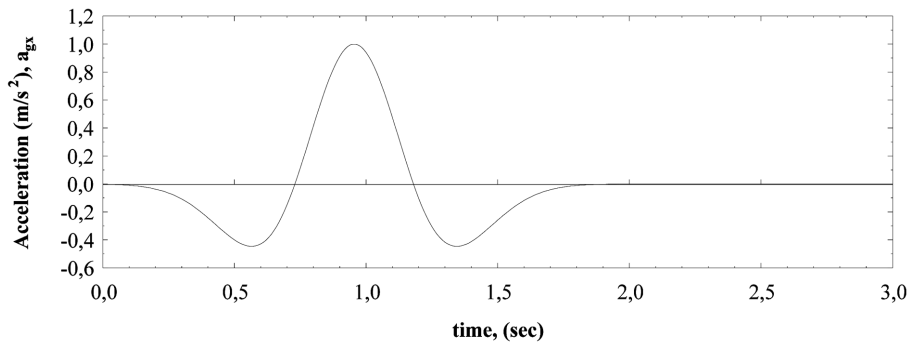


Fig. 4 Ricker-Wavelet signal

we carried out a comparative study and want to determine the effect of topographical irregularities and soil properties on the whole soil-structure system response relative to those of the reference system.

For the ground motion acceleration data acting horizontally on the soil-rigid base interface, Ricker-Wavelet is chosen. The input signal is shown in Fig. 4. Its equation in time is given as

$$f(t) = A_0(1 - 2a^2)e^{-a^2} \quad (11)$$

where $a = (t - t_s)/t_0$; t_s is the time at which the maximum occurs; A_0 is the amplitude and is fixed to 1, t_0 corresponds to the dominant period of the wavelet. In this study, t_0 was set to $1/\pi$, which corresponds to a dominant frequency of the wavelet near 1 Hz. The time lag t_s was taken equal to $3t_0$ ($t_s = 3/\pi$) as in Estorff *et al.* (1990).

In the parametric studies, a numerical procedure is employed to evaluate whole system response. In the numerical treatment, finite and infinite elements are used. For the discretization of the structure and the near soil region, standard eight-node isoparametric, quadratic plane finite elements are used. In the discretization of the far soil region, infinite elements that include three different wave types (P , S and Rayleigh waves) with a decay parameter are used. Some of the previous studies have shown that the effects of decay rates of different waves in the infinite elements are not

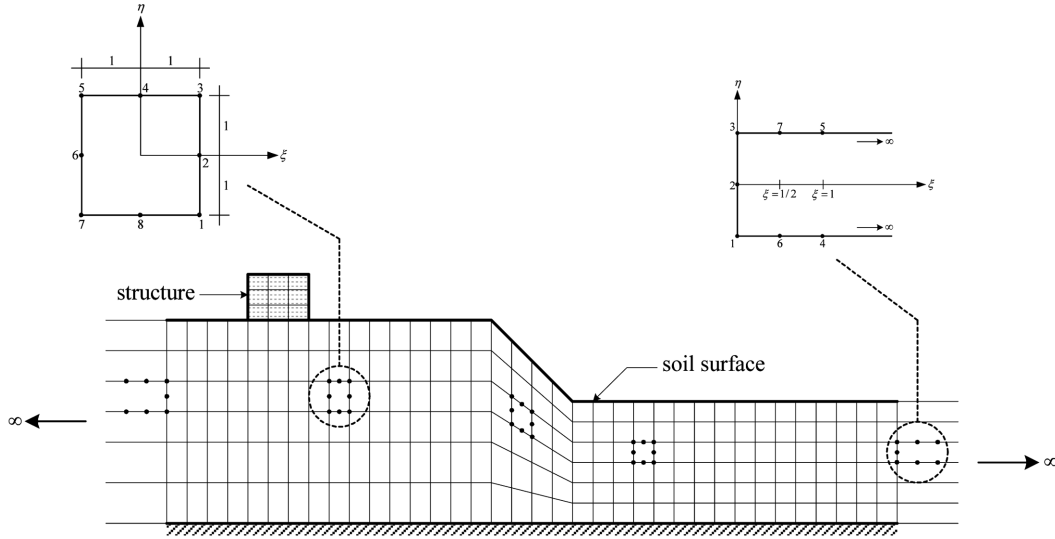


Fig. 5 Typical finite-infinite element discretization of the soil-structure systems

sensitive in the numerical analysis (Zhang and Zhao 1987). The shape functions of dynamic infinite elements are constructed by using a wave-propagation function that represents the amplitude attenuation and phase delay in the direction extending to infinity. Typical finite-infinite element discretization of the systems is shown in Fig. 5. For the finite and infinite elements presented earlier, a computer program coded in FORTRAN90 programming language is prepared. The efficiency and accuracy of the program code were published in Düzgün (2007). The solutions are obtained in the Laplace domain. Then using Durbin's numerical inverse Laplace transform technique (Durbin 1974), solutions are transformed into time domain.

In the analysis, relative horizontal displacements are computed at the top and bottom of the structure (points A and B) and upper and bottom edge of the slope (points C and D). Special attention is paid to evaluate the amplification of waves by the local soil properties and the amplification due to the topographical irregularities. Interest is focused on parameters determining dynamic behaviour of the soil-structure system under ground motion: location of the structure, slope angle (α) and soil properties. In this way, effects of these parameters on the system response are evaluated by comparing with those of the reference soil-structure system (T0). Displacements are calculated every 0.04 s. Maximal values of displacements, calculated in the time interval [0 s; 5.12 s] are considered. It should be noted that the results obtained from the parametric studies are relative quantities.

5. Results and discussion

Effects of surface shapes and soil properties on dynamic response of the soil-structure systems are evaluated. The general amplification mechanism due to topographic irregularities is reported in Gazetas *et al.* (2002) that the wave field affecting the surface motions consists of: (a) the vertically propagating incident SV wave; (b) waves reflecting at the horizontal ground surface and at the

sloping surface of the cliff; (c) waves transmitted through, and reflected at layer interfaces, and (d) diffracted waves. Diffracted waves include: (i) SP waves that are generated at the cliff surface due to the critical or near-critical incidence of the vertical SV waves. Such waves propagate upward along the sloping surface and interfere with direct SV waves; (ii) Rayleigh waves generated at the crest of the hill. The interference between these various types of direct and diffracted waves generates an increased motion near the crest and rapidly varying motion along the horizontal ground

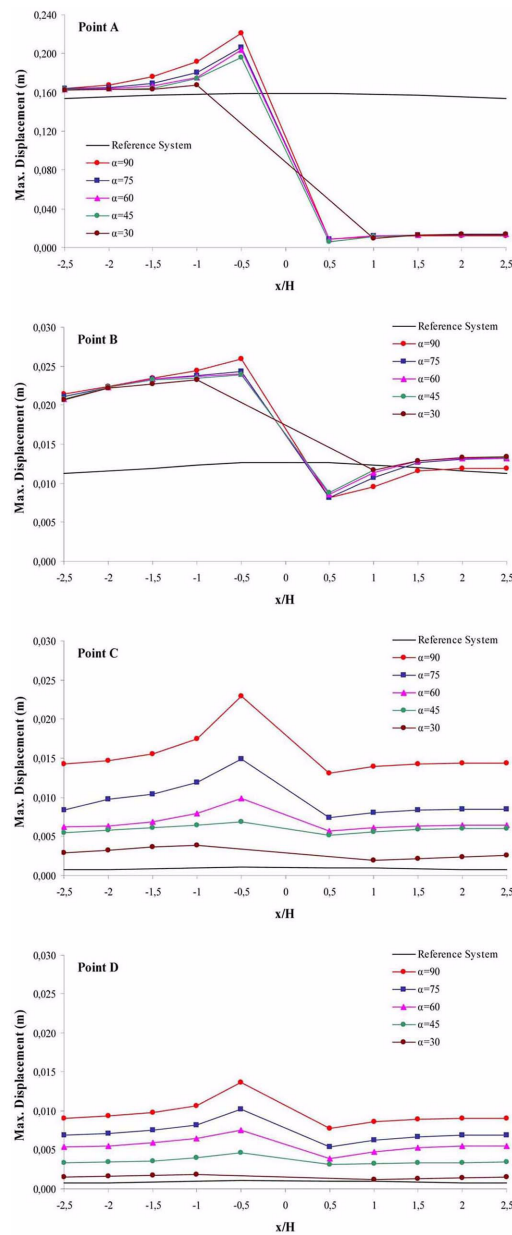


Fig. 6 Influence of topography on horizontal displacements for Soil Type I

surface. Although only one soil layer is taken into account, similar results are obtained in this study. Topographical effects are mainly caused by wave focusing in surface irregularities and inferences between incident and reflected plane waves with surface waves; however, amplification is affected by geological properties. According to the results obtained from the parametric studies, topographic features of a soil stratum have a significant influence on dynamic response of the soil-structure system. Soil properties and location of the structure have also a great influence on the system behaviour. The results also show that structures located at the top of irregular topographies, suffer more considerable damage than those located at the base. Moreover, structures standing near the edge of irregular topographies are affected more than those at some distance from the edge, in the event of a ground motion. Detailed results are drawn as below:

It is shown that surface shapes of the soil layer have a great influence on the dynamic response of the whole system, depending on the location of the structure. The results are summarized in Figs. 6-8 for different soil properties. According to the results, location of the structure is one of the parameters affecting dynamic response of the soil-structure system. In the reference system (T0), location of the structure has a minor effect on the system behaviour but in the other systems, i.e. $\alpha = 90^\circ$ (T1); $\alpha = 75^\circ$ (T2); $\alpha = 60^\circ$ (T3); $\alpha = 45^\circ$ (T4) and $\alpha = 30^\circ$ (T5), location of the structure is very effective on the whole system response. When location of the structure gets closer to the upper edge of the slope: the amplification of horizontal displacements at the upper and bottom sides of the structure (Points A and B) and the upper edge of the slope (Point C) increased, but at the bottom edge of the slope (Point D) slightly influenced, and so, horizontal displacements reached a local maximum near upper side of the slope. On the other hand, when the structure is located at the bottom side of the slope, smaller horizontal displacements are computed than those of the upper side of the slope. In this case, location of the structure has a minor effect on the system behaviour. The most critical case is when the structure located in the point which is the closest to the upper edge of the slope. However, surface shape of a soil stratum is another parameter affecting the system response. Site effects are reinforced by surface shapes. The results are summarized in Table 1, where U_{T0} , U_{T1} , U_{T2} , U_{T3} , U_{T4} and U_{T5} represent the maximal values of relative horizontal displacements of the soil-structure systems shown in Fig. 3, respectively. According to the results, the overall trends of amplification and attenuation are also strongly dependent on the surface geometry. Horizontal motions tend to be attenuated at the bottom side of the slope and amplified at the upper edges of the slope. Horizontal displacements decrease at bottom side of the slope, but increase at the upper side of the slope depend on the slope angle (α). When slope angle (α) gets

Table 1. Effects of slope angle (α) on the horizontal displacements for different soil properties relative to those of the reference system (T0)

	Soil Type I				Soil Type II				Soil Type III			
	A	B	C	D	A	B	C	D	A	B	C	D
U_{T0}/U_{T0}	1.00	1.00	1.00	1.00	1.00	1.00	1.00	1.00	1.00	1.00	1.00	1.00
U_{T1}/U_{T0}	1.39	2.04	22.05	13.16	1.35	1.74	32.26	15.52	1.27	1.74	24.70	11.52
U_{T2}/U_{T0}	1.30	1.92	14.35	9.82	1.26	1.70	22.54	11.94	1.21	1.69	18.69	9.25
U_{T3}/U_{T0}	1.28	1.90	9.43	7.29	1.24	1.67	16.03	8.97	1.17	1.68	14.67	6.98
U_{T4}/U_{T0}	1.23	1.88	6.61	4.48	1.21	1.65	10.47	5.33	1.16	1.68	12.04	3.98
U_{T5}/U_{T0}	1.06	1.88	4.13	1.96	1.06	1.63	4.55	1.82	1.06	1.66	4.99	1.03

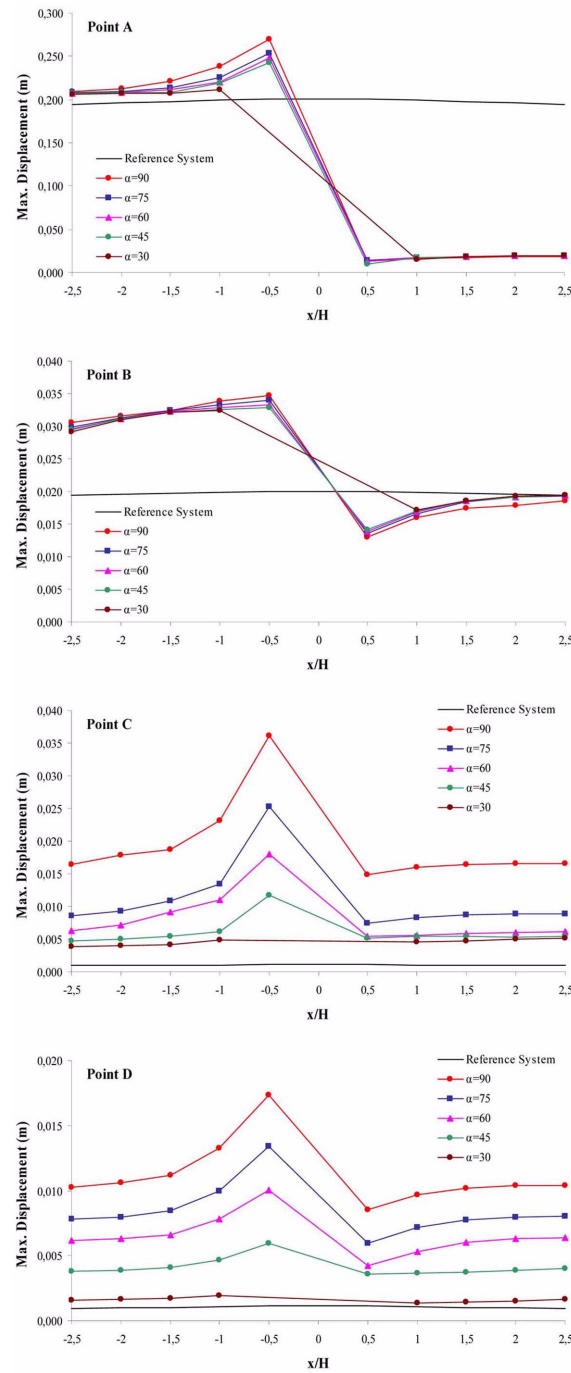


Fig. 7 Influence of topography on horizontal displacements for Soil Type II

greater, an amplification occurs at the upper and bottom sides of the structure (Points A and B) and at the upper and bottom edges of the slope (Points C and D). It is shown that for steeper slopes, the

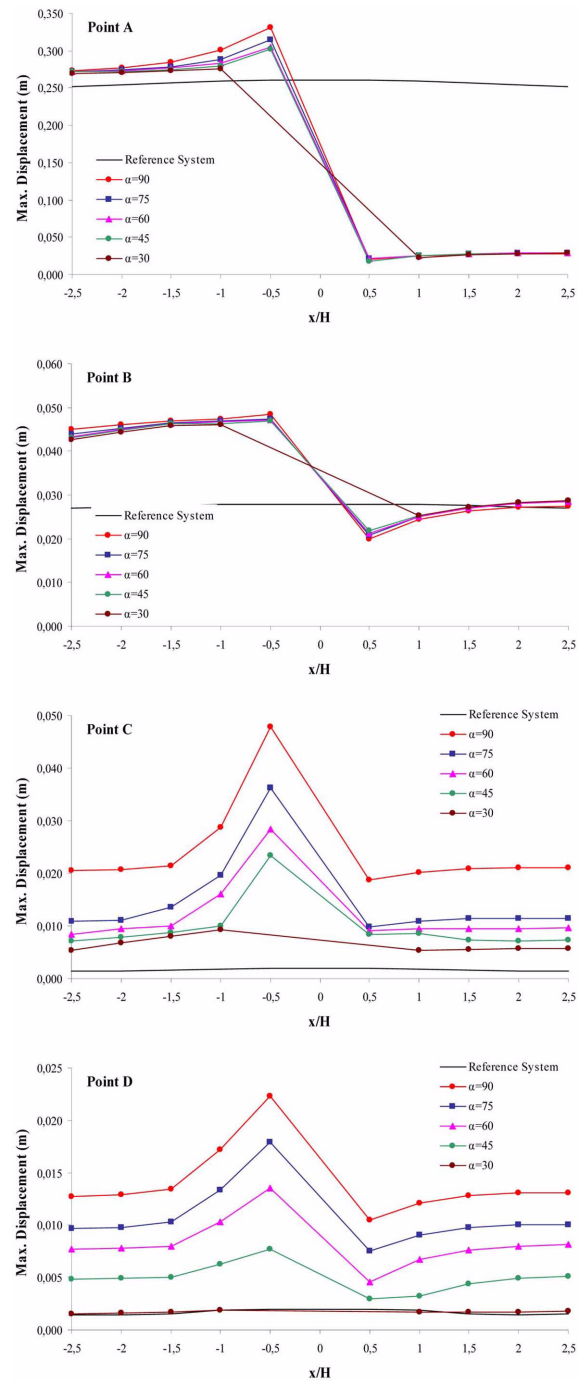


Fig. 8 Influence of topography on horizontal displacements for Soil Type III

amplification at the upper side and attenuation at the bottom side of the slope are accentuated. For reliefs of the same dimensions in plan, the system T0 is the least critical while the system T1 is the

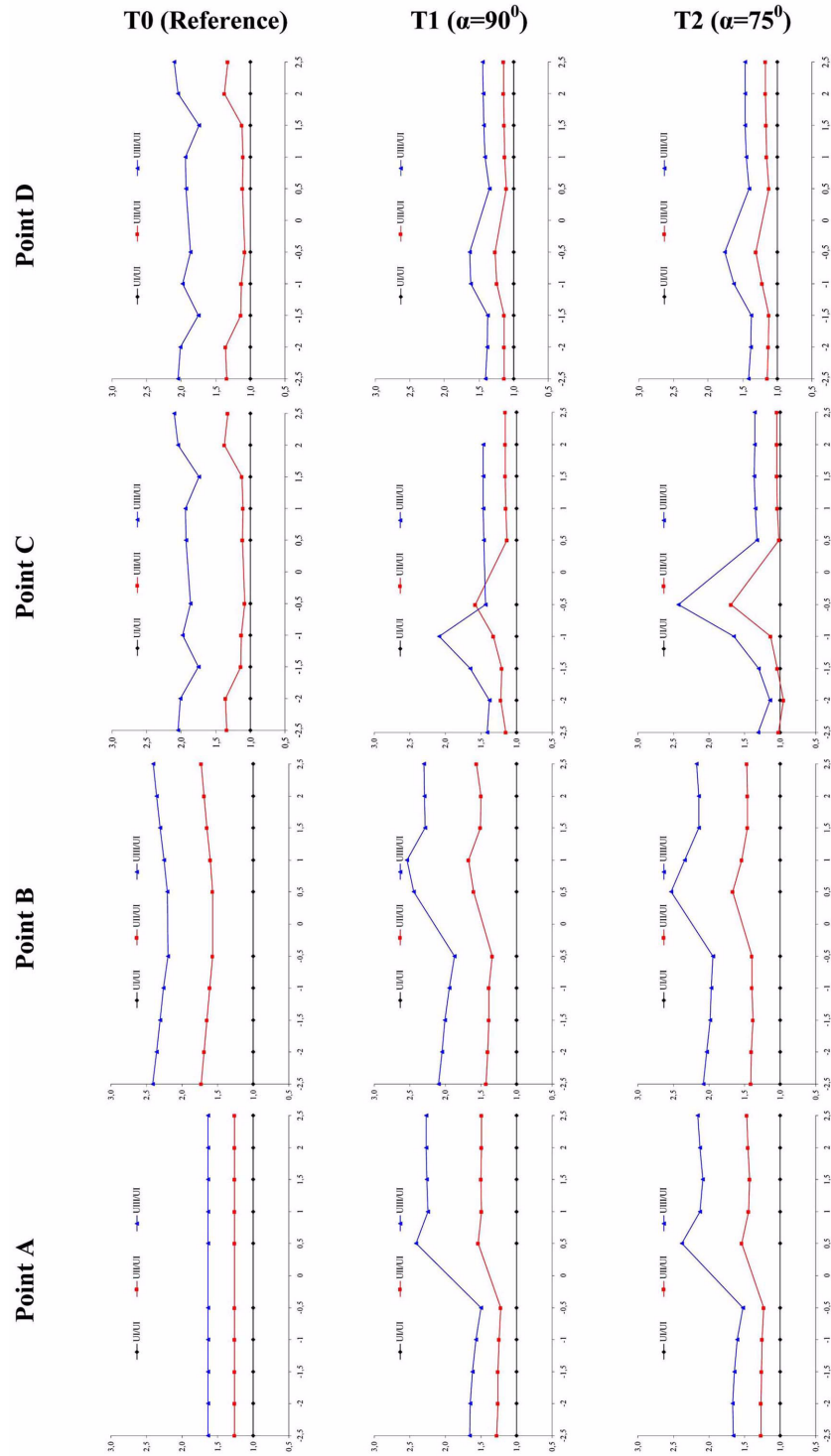


Fig. 9 Effects of soil properties on the horizontal displacements (horizontal axis represents x/H ratio; vertical axis represents displacement ratios)

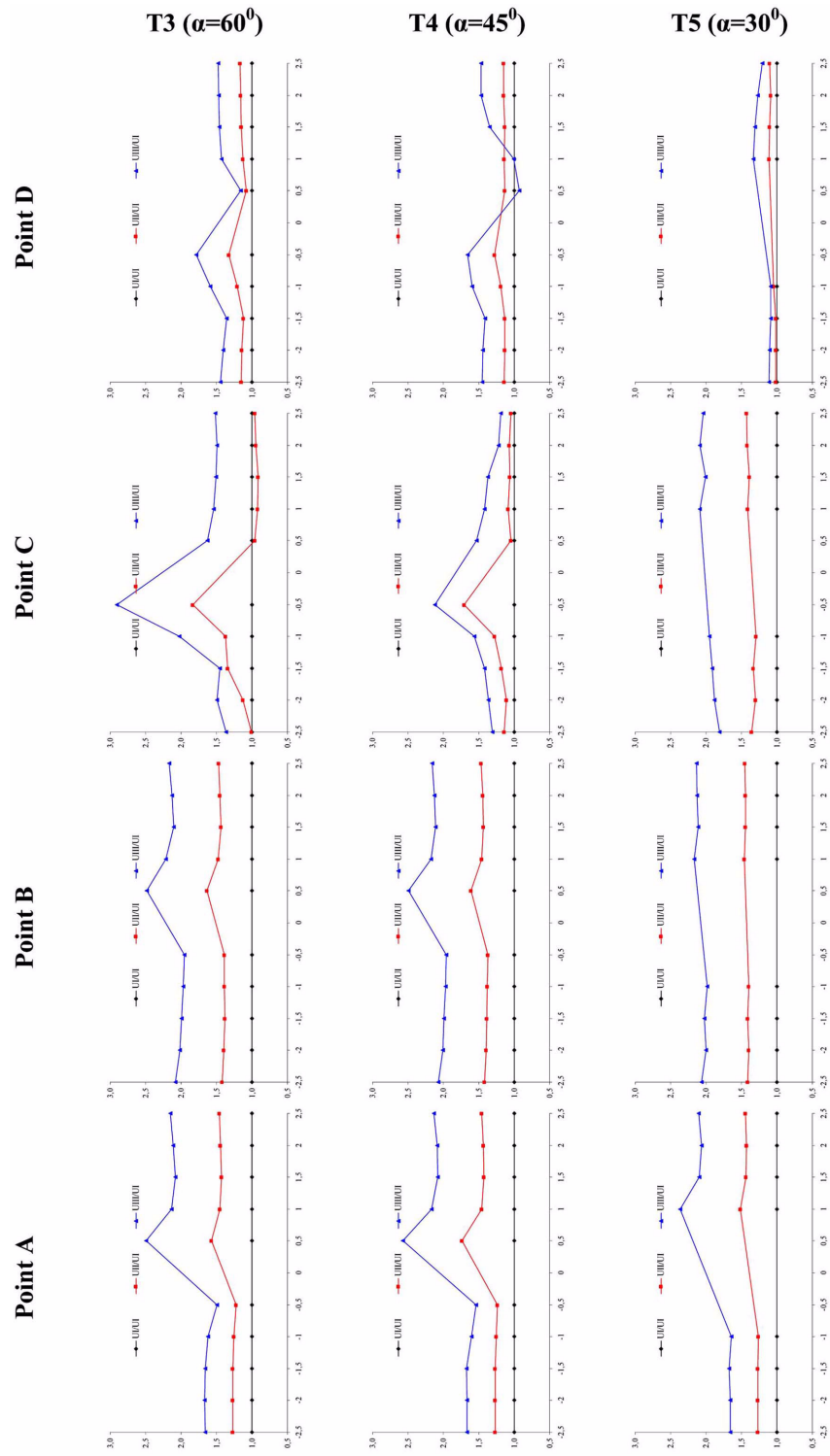


Fig. 9 (continued)

most critical case. Displacement amplifications got stronger as the slope became steeper i.e. the steeper the slope, the higher are site effects.

Geotechnical properties of the soil types are also effective on the whole soil-structure system response. In order to determine the effect of the geotechnical properties of the soil on the dynamic response of the soil-structure systems, three different soil types are studied, which correspond to dense, medium and loose soil properties, i.e., $G_1/G = 1$, $G_2/G = 0.75$ and $G_3/G = 0.5$, where G and $G\#$ represent the shear modulus of reference soil and of other soil types, respectively. Fig. 9 illustrates the effect of the soil properties on the dynamic response of the soil-structure systems, where U_I , U_{II} and U_{III} represent the relative horizontal displacements of the soil types: Soil Type I, Soil Type II and Soil Type III, respectively. The results show that horizontal motion of the systems is also affected by the geotechnical properties of the soil. According to the results, as the ratio $G\#/G$ decreases, i.e. the soil gets softer; the ratios U_{II}/U_I and U_{III}/U_I are increased. This fact indicates that the more intensive the softer soil types, the greater the amplification that can be expected, so the soft soils significantly aggravate the amplification and soil-structure interaction on stiff soils filters the horizontal motion. On the other hand, in general, maximal values for points A and B are obtained when the structure is located at the bottom side of the slope, while maximal values for points C and D are obtained when the structure is located at the upper side of the slope.

6. Conclusions

A parametric study is carried out for single-faced slopes to characterize topographical site effects by coupling finite and infinite elements with three wave types. Special attention is paid to evaluate the amplification of waves by the local soil properties and the amplification due to the topographical irregularities. Interest is focused on parameters determining dynamic behaviour of the soil-structure system under ground motion: location of the structure, soil properties and on slope angle (α). The results obtained in this study correspond with those in the literature. According to the results, dynamic response of a soil-structure system is affected by surface shapes, location of the structure and geotechnical properties of the soil. We have shown that: (i) it is shown that the effect of the surface shapes is strongly dependent on the on slope angle (α). Displacement amplifications got stronger as the slope became steeper i.e. the steeper the slope, the higher are site effects. (ii) location of the structure is also effective on the whole system response. When location of the structure gets closer to upper edge of the slope, the amplification of displacements increased. In this case, horizontal displacements reached a local maximum near upper side of the slope, but when the structure is located at the bottom side of the slope, location of the structure has a minor effect on the system behaviour. (iii) geotechnical properties of the soil are also effective on the displacement amplification. Soft soil layers significantly aggravate the amplitude of the motion, which cannot be neglected for design purposes, but as the soil became stiffer, the amplification decreased. (iv) weak motion data can be used as a guide in studies, but they are inadequate to describe topographical effects associated with real seismic events. (v) soil-structure interaction on stiff soil regions filters the horizontal motion. On the other hand, as the topographic irregularities of a soil-structure system are basically studied, the results might give an insight into or understanding of topographical effects of the single-faced slope.

References

- Assimaki, D., Kausel, E. and Gazetas, G. (2005), "Wave propagation and soil-structure interaction on a cliff crest during the 1999 Athens Earthquake", *Soil Dyn. Earthq. Eng.*, **25**, 513-527.
- Avilés, J. and Pérez-Rocha, L.E. (1998), "Site effects and soil-structure interaction in the Valley of Mexico", *Soil Dyn. Earthq. Eng.*, **17**, 29-39.
- Bettess, P. and Zienkiewicz, O.C. (1977), "Diffraction and refraction of surface waves using finite and infinite elements", *Int. J. Numer. Meth. Eng.*, **11**, 1271-1290.
- Boore, D.M. (1972), "A note on the effect of simple topography on seismic SH waves", *B. Seismol. Soc. Am.*, **62**, 275-284.
- Celebi, M. (1987), "Topographical and geological amplifications determined from strong-motion and aftershock records of the 3 March 1985 Chile earthquake", *B. Seismol. Soc. Am.*, **77**, 1147-1157.
- Chávez-García, F.J. and Faccioli, E. (2000), "Complex site effects and building codes: making the leap", *J. Seismol.*, **4**, 23-40.
- Chore, H.S., Ingle, R.K. and Sawant W.A. (2010), "Building frame-pile foundation-soil interaction analysis: a parametric study", *Int. Multiscale Mech.*, **3**, 55-79.
- Durbin, F. (1974), "Numerical inversion of Laplace transforms: an efficient improvement to Dubner and Abate's method", *Comput. J.*, **12**(4), 371-376.
- Düzgün, O.A. (2007), "Effects of Topography on the Dynamic Response of Soil Structure Systems", PhD thesis, Graduate School of Natural and Applied Sciences, Department of Civil Engineering, Atatürk University, Erzurum, Turkey (In Turkish).
- Estorff, O., Pais, A.L. and Kausel, E. (1990), "Some observations on time domain and frequency domain boundary elements", *Int. J. Numer. Meth. Eng.*, **29**, 785-800.
- Gatmiri, B. and Arson, C. (2008), "Seismic site effects by an optimized 2D BE/FE method II. Quantification of site effects in two-dimensional sedimentary valleys", *Soil Dyn. Earthq. Eng.*, **28**(8), 646-661.
- Gazetas, G., Kallou, P.V. and Psarropoulos, P.N. (2002), "Topography and soil effects in the M_s 5.9 Parnitha (Athens) earthquake: the case of Adámes", *Natur. Hazard.*, **27**, 133-169.
- Havenith, H.B., Vanini, M., Jongmans, D. and Faccioli, E. (2003), "Initiation of earthquake-induced slope failure: influence of topographical and other site specific amplification effects", *J. Seismol.*, **7**, 397-412.
- Kawase, H. and Aki, K. (1990), "Topography effect at the critical SV wave incidence: Possible explanation of damage pattern by the Whittier-Narrows, California, earthquake of 1 October 1987", *B. Seismol. Soc. Am.*, **80**, 1-22.
- LeBrun, B., Hatzfeld, D., Bard, P.Y. and Bouchon, M. (1999), "Experimental study of the ground motion on a large scale topographical hill at Kitherion (Greece)", *J. Seismol.*, **3**, 1-15.
- Ohtsuki, A. and Harumi, K. (1983), "Effect of topography and subsurface inhomogeneities on seismic SV waves", *Earthq. Eng. Struct. D.*, **11**, 441-462.
- Ohtsuki, A., Yamahara, H. and Harumi, K. (1984), "Effect of topography and subsurface inhomogeneity on seismic Rayleigh waves", *Earthq. Eng. Struct. D.*, **12**, 37-58.
- Reddy, J.N. (1993), "An Introduction to the Finite Element Method", *McGraw-Hill International Editions, Engineering Mechanics Series*, Singapore.
- Stewart, J.P. and Sholtis, S.E. (2005), "Case study strong ground motion variations across cut slope", *Soil Dyn. Earthq. Eng.*, **25**, 539-545.
- Trifunac, M.D. (1973), "Scattering of plane SH waves by a semi-cylindrical canyon", *Earthq. Eng. Struct. D.*, **1**, 267-281.
- Wong, H.L. and Trifunac, M.D. (1974), "Scattering of plane SH waves by a semi-elliptical canyon", *Earthq. Eng. Struct. D.*, **3**, 157-169.
- Wong, H.L. and Jennings, P.C. (1975), "Effect of canyon topography on strong ground motion", *B. Seismol. Soc. Am.*, **65**(5), 1239-1257.
- Wong, H.L., (1979), "Diffraction of P, SV and Rayleigh waves by surface topographies", University of Southern California, Department of Civil Engineering, Report No: CE 79-05, Los Angeles, California, USA.
- Yerli, H.R., Temel, B. and Kiral, E. (1998), "Transient infinite elements for 2D soil-structure interaction analysis", *J. Geotech. Geoenviron.*, **124**(10), 976-988.

- Zhang, C.H. and Zhao, C.B. (1987), "Coupling method of finite and infinite elements for strip foundation wave problems", *Earthq. Eng. Struct. D.*, **15**, 839-851.
- Zhang, C.H. and Zhao, C.B. (1988), "Effects of canyon topography and geological conditions on strong ground motion", *Earthq. Eng. Struct. D.*, **16**, 81-97.
- Zulkifli, E. and Ruge, P. (2009), "Transient soil-structure interaction with consistent description of radiation damping", *Struct. Eng. Mech.*, **33**, 47-66.